Multiband TOA Positioning Technique Using an UHF Bandwidth Availability Model for Cognitive Radio

R. R. Thomas*, B.T. Maharaj*, B. Zayen† and R. Knopp†

*Department of Electrical, Electronic and Computer Engineering,

University of Pretoria, Pretoria, South Africa

Email: robinthomas@ieee.org, sunil.maharaj@up.ac.za

†Mobile Communications Department, EURECOM Sophia Antipolis, France

Email: {bassem.zayen,raymond.knopp}@eurecom.fr

Abstract

In this paper, the authors present a multiband time-of-arrival (TOA) positioning model and validate the performance in a practical dynamic spectrum access scenario according to results obtained from an ultra-high frequency (UHF) spectrum occupancy measurement campaign. The statistical analysis of the measured data shows a distinguishable difference between the unoccupied and occupied portion of the UHF band. The bandwidth availability for the UHF band is shown to follow a Gaussian distribution according to the measurement results. The positioning model is verified using the non-linear least squares, linear least squares and two-step maximum-likelihood location estimation algorithms. The root mean square error (RMSE) performance evaluation of the proposed model revealed the advantage of utilising five discrete bands to perform TOA estimation, especially in poor signal-to-noise ratio (SNR) conditions ranging from -10 dB to 0 dB. At a fixed SNR of 0 dB, an average RMSE improvement of 74% and 82% was observed for a double and triple band system when compared to a conventional single-band TOA system. This particular positioning technique can enable improved location estimation in a dynamic spectrum access environment.

Index Terms- bandwidth availability, cognitive radio, linear least squares, multiband time-of-arrival positioning, non-linear least squares, two-step maximum-likelihood, UHF measurement campaign

I. Introduction

Cognitive radio has been regarded as the next evolution in wireless communications in anticipation of the spectrum shortage and lack of efficient usage by telecommunication operators (also referred to as primary users). It has been shown through various measurement campaigns conducted by regulatory bodies and research institutes that significant portions of the radio frequency spectrum are under-utilised while other portions of the spectrum, such as the Global System for Communication (GSM) band, are highly congested [1], [2]. Currently there is no provision for secondary users (SUs)(or unlicensed users) to utilise the unused portions (white spaces) of the spectrum in a non-interfering manner with primary users (PUs) in the current fixed spectrum allocation. One of cognitive radio's capabilities includes the dynamic utilisation of these white spaces through artificial intelligence, adaptation and awareness. There are a number of enabling technologies for cognitive radio. One such technology is the ability to gather and maintain accurate location awareness of the surroundings, as well as the current state of the spectrum. Currently, there are a variety of localisation technologies such as Global Positioning Satellites (GPS), cellular-aided positioning as well as cooperative techniques. The missing feature in each of these current positioning technologies is the ability to adapt, especially according to bandwidth availability. Applications which can be improved and optimised through location-aided data include dynamic spectrum management, dynamic channel allocation algorithms, autonomous network expansion procedures, handover algorithms and adaptive coverage systems [3]. Receiver location information has become an integral part of the IEEE 802.22 working standard for Wireless Regional Area Networks (WRAN) [4]. A key feature of this standard includes dynamic spectrum access, which is performed by using energy detection and the geo-location information of the base station and user, to perform dynamic channel allocation in the very high frequency (VHF) and ultra-high frequency (UHF) bands. In addition, knowledge of a cognitive radio user's location data also plays an important role in setting up transmission protocols for spectrum-efficient communications [5].

The Cognitive Positioning System (CPS) proposed in [6] uses a combination of adaptive bandwidth selection as well as dynamic spectrum allocation techniques to address the location awareness requirements of cognitive radio. Time-based ranging schemes such as time-of-arrival (TOA) or time-difference-of-arrival (TDOA) are particularly suited for localisation systems employing ultra-wideband (UWB) or orthogonal frequency division multiplexing (OFDM) in cognitive radio, since the bandwidth and signal-to-noise ratio (SNR) of the ranging signal affect the positional accuracy (location estimate) of the receiver [7]. Previous works [8], [9] have shown that conventional TOA ranging is a suitable technique for single-band positioning systems. It has also been shown that optimal two-step time-delay estimation can be conducted simultaneously on dispersed bands for cognitive radio systems using a variety of combining schemes, each with different degrees of performance under various modulation schemes [10], [11]. To the best of the authors' knowledge, there has been no previous work that has investigated the positional accuracy of multiband TOA location estimation in the context of a dynamic bandwidth availability model based on empirical results.

In a typical dynamic spectrum access scenario, it is envisioned that multiple white spaces (spectrum holes) can be opportunistically accessed by SUs (using cognitive radio devices) to perform TOA location estimation in addition to performing voice and data communications. This paper addresses an analytical approach for performing improved two-dimensional (2D) location estimation using multiple TOA signals. The derivation of a generalised Cramer-Rao lower bound (CRLB) time delay and channel coefficient estimate is presented in order to develop an effective combining estimation technique for the multiband TOA system, which serves to improve the positional accuracy performance over a single-band TOA system. This derivation also achieves adaptivity using the bandwidth and positional accuracy relationship. In a practical dynamic spectrum access environment, multiple signal bandwidths may not always be available to perform TOA location estimation, since these signals might be utilised by PUs. Therefore using results from a UHF measurement campaign a probabilistic model was created in order to describe the availability of these multiple bandwidths. An SU would then exploit these available bandwidths using cognitive radio to perform more accurate TOA location estimation as opposed

to an SU that would only utilise a single available bandwidth to perform TOA location estimation. The performance of the multiband TOA system was analysed using the non-linear least squares estimation (NLS), linear least squares (LLS) and two-step maximum-likelihood (TSML) location estimation algorithms, as each of these algorithms has its own tradeoff in terms of complexity and estimation accuracy. This proposed positioning technique has been developed in the context of future application in various multicarrier communication standards, most of which, are fundamentally based on OFDM such as LTE, DVB-T2 and WiMax etc.[12].

The rest of the paper is organised as follows: In Section II an overview of the system signal model is provided. Section III provides the generalised CRLB estimate of the time delay and channel coefficient for each signal of the multiband system in order to develop a suitable combining estimation technique. Thereafter, in Section IV, the CRLB is derived for a special case where a single time delay estimate is to be computed across multiple signals in order to show that the adaptivity feature is necessary for multiband TOA systems. In Section V, the spectrum occupancy measurement results are discussed where a model for dynamic bandwidth availability is developed by determining the probability density function (PDF) of the unoccupied and occupied portions of the UHF band. The simulated results of the multiband TOA system are provided in Section VI, while Section VII draws the main conclusions of this study.

II. Multiband Signal Model

The mathematical signal model for deriving the CRLB and required estimates forms the initial basis of this study. This model tackles the case of a line-of-sight single-path scenario, where there is a direct path between the anchor nodes (base stations) and the target node (mobile terminal). As a result, the delay of the strongest path is considered. Analysis of multiple signals each with multipath components can drastically increase the complexity of the problem at hand and therefore can be considered for future work. Let the baseband representation of each received signal ($r(t)$) within the multiband model be represented as:

$$r_i(t) = \alpha_i s_i(t - \tau_i) + n_i(t), \quad 0 \leq t \leq T,\ i \in [1..N], \tag{1}$$

where α_i represents the complex channel fading coefficient of each signal identified by i for a total of N signals, $s_i(t-\tau_i)$ is the delayed transmitted signal occupying a specific bandwidth (β_i) and $n_i(t)$ represents a zero mean additive white Gaussian noise (AWGN) process with variance, σ_i^2. The assumption is made that over the interval between 0 and T_s (symbol time), the transmitted pulse given by $s(t)$ is non-zero and band-limited to a frequency of B Hz. As a result the observation interval encompasses the symbol time and maximum time delay, which can also be shown as follows: $T = T_s + \tau_{max}$. The equivalent frequency domain representation of (1) is provided:

$$R_i(\omega) = S_i(\omega)\alpha_i e^{(-j\omega\tau_i)} + N_i(\omega), \tag{2}$$

where $S_i(\omega)$ and $N_i(\omega)$ are the Fourier transform representations of the transmitted and AWGN signals respectively:

$$S_i(\omega) = \mathcal{F}\{s_i(t)\} = \int_0^{1/T} s_i(t)e^{(-j\omega t)}dt, \tag{3}$$

$$N_i(\omega) = \mathcal{F}\{n_i(t)\} = \int_0^{1/T} n_i(t)e^{(-j\omega t)}dt, \tag{4}$$

where $\mathcal{F}$ is the Fourier transform operator. The Fourier transform parameter is given by $\omega = 2\pi f$, where f represents frequency. Fig. 1 displays the proposed receiver model for the multiband TOA positioning system where $\hat{\beta}_1, ..., \hat{\beta}_N$ represents the bandwidth of each received signal. The time delay and channel coefficients are evaluated separately and then utilised to perform 2D location estimation of an SU (also referred to as the target node).

The time delay and channel coefficient estimate from each ranging signal is simultaneously extracted through parallel signal processing at the receiver front-end. The main advantage is that the varying bandwidths of multiple ranging signals are exploited to obtain an improved location estimate by combining all the time delays. The combining technique utilises the CRLB estimate of each band to enable adaptivity and yield an overall improved time delay estimate for enhanced TOA ranging.

III. Time delay and channel coefficients combining estimation technique

The general CRLB of the time delay and channel coefficient estimates can be derived according to the multiband signal model represented in (1). The vector representation of the required parameters to be estimated can therefore be given as [13]:

$$\boldsymbol{\Theta}_i = [\tau_i \quad \alpha_i], \tag{5}$$

where τ_i is the signal time delay and α_i represents the complex channel coefficients corresponding to a single-band, which describes the fading of each received signal. The CRLB is given by the first row and first column of an inverse matrix as shown by the following relationship [14]:

$$var(\hat{\boldsymbol{\Theta}}_i) \geq \left[\mathbf{I}^{-1}(\boldsymbol{\Theta})\right]_{ii}, \tag{6}$$

where $\mathbf{I}(\boldsymbol{\Theta})$ is a $q \times q$ Fisher Information Matrix (FIM) and q is defined by the number of unknown parameters to estimate. In this case, $\Theta_1 = \tau_i$ and $\Theta_2 = \alpha_i$. The elements of the 2×2 FIM have been determined for a general Gaussian case for a discrete received signal using:

$$\mathbf{I}(\boldsymbol{\Theta}) = \frac{1}{\sigma_i^2} \sum_{k=0}^{K-1} \frac{\partial s_i[k;\boldsymbol{\Theta}]}{\partial \boldsymbol{\Theta}_i} \frac{\partial s_i[k;\boldsymbol{\Theta}]}{\partial \boldsymbol{\Theta}_j} \tag{7}$$

where $i = 1, 2, .., q$ and $j = 1, 2, ..., q$.
This results in a 2×2 FIM given by:

$$\mathbf{I}(\boldsymbol{\Theta}_i) = \begin{bmatrix} I_{\tau_i\tau_i} & I_{\tau_i\alpha_i} \\ I_{\alpha_i\tau_i} & I_{\alpha_i\alpha_i} \end{bmatrix}. \tag{8}$$

The following FIM elements can be derived using (7)[13]:

$$I_{\tau_i\tau_i} = \frac{|\alpha_i|^2 \hat{\varepsilon}_i}{\sigma_i^2}, \tag{9}$$

$$I_{\tau_i\alpha_i} = I_{\alpha_i\tau_i} = -\frac{|\alpha_i| \tilde{\varepsilon}_i}{\sigma_i^2}, \tag{10}$$

$$I_{\alpha_i\alpha_i} = \frac{\varepsilon_i}{\sigma_i^2}, \tag{11}$$

where $\hat{\varepsilon}_i$ and $\tilde{\varepsilon}_i$ are respectively given as:

$$\hat{\varepsilon}_i = \int_0^T \left|\tilde{\lambda}\right|^2 dt, \tag{12}$$

$$\tilde{\varepsilon}_i = \int_0^T |\tilde{\lambda}||\lambda| dt. \tag{13}$$

The first derivative of the signal energy λ is given by $\tilde{\lambda} = s_i'(t-\tau)$, while the energy ($\varepsilon_i$) of the signal $\lambda = s_i(t-\tau)$ is shown as:

$$\varepsilon_i = \int_0^T |s_i(t-\tau)|^2 dt. \tag{14}$$

The CRLB of the time delay estimate can be obtained using the following matrix algebraic manipulation:

$$[I_{\tau_i\tau_i}]^{-1} = \left(I_{\tau_i\tau_i} - I_{\tau_i\alpha_i} I_{\alpha_i\alpha_i}^{-1} I_{\alpha_i\tau_i}\right)^{-1}. \tag{15}$$

Therefore, the CRLB of the time delay estimate for an individual band is given as:

$$\begin{aligned}
[I_{\tau_i\tau_i}]^{-1} &= \frac{|\alpha_i|^2\hat{\varepsilon}_i}{\sigma_i^2} - \frac{|\alpha_i|\tilde{\varepsilon}_i}{\sigma_i^2} \times \frac{\sigma_i^2}{\varepsilon_i} \times \frac{|\alpha_i|\tilde{\varepsilon}_i}{\sigma_i^2} \\
&= \frac{|\alpha_i|^2}{\sigma_i^2}\left(\hat{\varepsilon}_i - \frac{\tilde{\varepsilon}_i^2}{\varepsilon_i}\right) \\
&= var\left(\hat{\tau}_i\right)^{-1} = c^2 P(\hat{d}).
\end{aligned} \tag{16}$$

Using (16), it is possible to derive a relationship between the CRLB time-delay estimate and the positional accuracy of the target node (TN) [6]:

$$var(\hat{\tau}) = \frac{1}{c^2 P(\hat{d})}, \tag{17}$$

where c is the speed of light and $P(\hat{d})$ is the positional accuracy of the TN. The bandwidth

representation using the Fourier transform can be expressed as:

$$\hat{\varepsilon}_i = \varepsilon_i \hat{\beta}_i^2, \tag{18}$$

where the bandwidth of the signal $(s_i(t))$ in the frequency domain $(S_i(\omega))$ is given by [15]:

$$\hat{\beta}_i^2 = \frac{\int_{-\infty}^{\infty} \omega^2 |S_i(\omega)|^2 d\omega}{\int_{-\infty}^{\infty} |S_i(\omega)|^2 d\omega}. \tag{19}$$

Using (16) and (18), one can obtain a bandwidth determination equation based on the required positional accuracy of the TN, which can be adapted based on the availability of the required number of bands:

$$\begin{aligned} \frac{|\alpha_i|^2}{\sigma_i^2}\left(\hat{\varepsilon}_i - \frac{\tilde{\varepsilon}_i^2}{\varepsilon_i}\right) &= c^2 P(\hat{d}) \\ \frac{|\alpha_i|^2}{\sigma_i^2}\left(\varepsilon_i \hat{\beta}_i^2 - \frac{\tilde{\varepsilon}_i^2}{\varepsilon_i}\right)^2 &= c^2 P(\hat{d}) \\ \varepsilon_i \hat{\beta}_i^2 &= \frac{c^2 P(\hat{d}) \sigma_i^2}{|\alpha_i|^2} + \frac{\tilde{\varepsilon}_i^2}{\varepsilon_i} \\ \hat{\beta}_i &= \sqrt{\frac{c^2 P(\hat{d}) \sigma_i^2}{|\alpha_i|^2 \varepsilon_i} + \frac{\tilde{\varepsilon}_i^2}{\varepsilon_i^2}}. \end{aligned} \tag{20}$$

It can be noted that the derivative of the signal energy is zero, which results in $\tilde{\varepsilon} = 0$. The estimated required bandwidth for a specified positional accuracy is given as:

$$\hat{\beta}_i = \sqrt{\frac{c^2 P(\hat{d})}{|\alpha_i|^2 \zeta_i}}, \tag{21}$$

where ζ_i is the SNR of the received signal. The CRLB of the channel coefficient estimate for an individual band is calculated using:

$$[I_{\alpha_i \alpha_i}]^{-1} = \left(I_{\alpha_i \alpha_i} - I_{\alpha_i \tau_i} I_{\tau_i \tau_i}^{-1} I_{\tau_i \alpha_i}\right)^{-1}. \tag{22}$$

This leads to the following CRLB for the channel coefficient estimate:

$$\begin{aligned}[I_{\alpha_i\alpha_i}]^{-1} &= \frac{\varepsilon_i}{\sigma_i^2} - \frac{\tilde{\varepsilon}_i^2}{\sigma_i^2\hat{\varepsilon}_i} \\ &= \frac{1}{\sigma_i^2}\left(\varepsilon_i - \frac{\tilde{\varepsilon}_i^2}{\hat{\varepsilon}_i}\right) \\ &= var\left(\hat{\alpha}_i\right)^{-1}. \end{aligned} \tag{23}$$

Two combining estimation techniques were investigated. The first method involved the averaging of the delay estimates over the total number of bands and the second method involved determining the minimum estimate over all the discrete bandwidths. An improved estimate between the two combining techniques was shown to be given by the latter method. It can therefore be noted that the channel coefficient and SNR of the received signal, together with the total number of bands, are important parameters which affect the accuracy of the TOA location estimate.

IV. CRLB OF OVERALL TIME DELAY AND CHANNEL COEFFICIENT ESTIMATES

Section III provided the CRLB of the time delay estimate and channel coefficient estimate of each individual signal in order to derive an appropriate combination estimation technique. The overall multiband system is investigated for the special case where a single time delay is estimated and this analysis ascertains whether adaptation of bandwidth and positional accuracy is possible. In this particular case, the signal delay (τ) has also been assumed to be constant for all transmitted signals. Accordingly the following vector of unbiased signal parameters have to be estimated:

$$\boldsymbol{\Theta} = [\tau \quad \boldsymbol{\alpha}], \tag{24}$$

where τ is the signal time delay and $\boldsymbol{\alpha} = [\alpha_1 ... \alpha_N]$ represents the vector of complex channel coefficients corresponding to N bands.The FIM is therefore represented as:

$$\mathbf{I}(\boldsymbol{\Theta}) = \begin{bmatrix} I_{\tau\tau} & \mathbf{I}_{\tau\boldsymbol{\alpha}} \\ \mathbf{I}_{\boldsymbol{\alpha}\tau} & \mathbf{I}_{\boldsymbol{\alpha}\boldsymbol{\alpha}} \end{bmatrix}. \tag{25}$$

In a similar fashion to Section III, each FIM element is computed using:

$$\mathbf{I}(\mathbf{\Theta}) = \sum_{i=1}^{N} \frac{1}{\sigma_i^2} \sum_{k=0}^{K-1} \frac{\partial s_i[k;\mathbf{\Theta}]}{\partial \mathbf{\Theta}_i} \frac{\partial s_i[k;\mathbf{\Theta}]}{\partial \mathbf{\Theta}_j}. \tag{26}$$

As a result, the FIM elements for this particular 2×2 case are as follows:

$$I_{\tau\tau} = \sum_{i=1}^{N} \frac{|\alpha_i|^2 \hat{\varepsilon}_i}{\sigma_i^2}, \tag{27}$$

$$\mathbf{I}_{\tau\boldsymbol{\alpha}} = \mathbf{I}_{\boldsymbol{\alpha}\tau}^T = -\left[\frac{|\alpha_1|\tilde{\varepsilon}_1}{\sigma_1^2}, ..., \frac{|\alpha_N|\tilde{\varepsilon}_N}{\sigma_N^2}\right], \tag{28}$$

$$\mathbf{I}_{\boldsymbol{\alpha}\boldsymbol{\alpha}} = diag\left[\frac{\varepsilon_1}{\sigma_1^2}, ..., \frac{\varepsilon_N}{\sigma_N^2}\right]. \tag{29}$$

The CRLB of the time delay estimate can be computed in a similar way to (15), bearing in mind that in this case, vector elements are involved:

$$[I_{\tau\tau}]^{-1} = \left(I_{\tau\tau} - \mathbf{I}_{\tau\boldsymbol{\alpha}}\mathbf{I}_{\boldsymbol{\alpha}\boldsymbol{\alpha}}^{-1}\mathbf{I}_{\boldsymbol{\alpha}\tau}\right)^{-1}, \tag{30}$$

and similarly the channel coefficients can be computed as follows:

$$[\mathbf{I}_{\boldsymbol{\alpha}\boldsymbol{\alpha}}]^{-1} = \left(\mathbf{I}_{\boldsymbol{\alpha}\boldsymbol{\alpha}} - \mathbf{I}_{\boldsymbol{\alpha}\tau}I_{\tau\tau}^{-1}\mathbf{I}_{\tau\boldsymbol{\alpha}}\right)^{-1}. \tag{31}$$

The time delay estimate of the signal is determined using (30) and is given by:

$$
\begin{aligned}
[I_{\tau\tau}]^{-1} =& \sum_{i=1}^{N} \frac{|\alpha_i|^2 \hat{\varepsilon}_i}{\sigma_i^2} - \left[\frac{|\alpha_1|\tilde{\varepsilon}_1}{\sigma_1^2}, ..., \frac{|\alpha_N|\tilde{\varepsilon}_N}{\sigma_N^2}\right] \\
& \times diag\left[\frac{\varepsilon_1}{\sigma_1^2}, ..., \frac{\varepsilon_N}{\sigma_N^2}\right]^{-1} \times \begin{bmatrix} \frac{|\alpha_1|\tilde{\varepsilon}_1}{\sigma_1^2} \\ \vdots \\ \frac{|\alpha_N|\tilde{\varepsilon}_N}{\sigma_N^2} \end{bmatrix} \\
=& \sum_{i=1}^{N} \frac{|\alpha_i|^2 \hat{\varepsilon}_i}{\sigma_i^2} - \left[\frac{\tilde{\varepsilon}_1|\alpha_1|}{\varepsilon_1}, ..., \frac{\tilde{\varepsilon}_N|\alpha_N|}{\varepsilon_N}\right] \times \begin{bmatrix} \frac{\tilde{\varepsilon}_1|\alpha_1|}{\sigma_1^2} \\ \vdots \\ \frac{\tilde{\varepsilon}_N|\alpha_N|}{\sigma_N^2} \end{bmatrix} \\
=& \sum_{i=1}^{N} \frac{|\alpha_i|^2}{\sigma_i^2} \left(\hat{\varepsilon}_i - \frac{\tilde{\varepsilon}_i^2}{\varepsilon_i}\right) \qquad (32) \\
=& var\left(\hat{\tau}\right)^{-1}. \qquad (33)
\end{aligned}
$$

It can be noted that the overall estimated time-delay is dependent on the channel coefficient for each band. Using similar methods in Section III, the positional accuracy is shown to be:

$$
P(\hat{d}) = \frac{1}{c^2} \sum_{i=1}^{N} \frac{|\alpha_i|^2}{\sigma_i^2} \left(\varepsilon_i \hat{\beta}_i^2 - \frac{\tilde{\varepsilon}_i^2}{\varepsilon_i}\right). \qquad (34)
$$

It can be also shown that the CRLB estimate of the channel coefficient for all dispersed bands can be computed using (31):

$$
\begin{aligned}
[\mathbf{I}_{\boldsymbol{\alpha\alpha}}]^{-1} &= diag\left[\frac{\varepsilon_1}{\sigma_1^2}, ..., \frac{\varepsilon_N}{\sigma_N^2}\right] - \left[\frac{|\alpha_1|\tilde{\varepsilon}_1}{\sigma_1^2}, ..., \frac{|\alpha_N|\tilde{\varepsilon}_N}{\sigma_N^2}\right] \times \left(\sum_{i=1}^{N} \hat{\varepsilon}_i \frac{|\alpha_i|^2}{\sigma_i^2}\right)^{-1} \times \begin{bmatrix} \frac{|\alpha_1|\tilde{\varepsilon}_1}{\sigma_1^2} \\ \vdots \\ \frac{|\alpha_N|\tilde{\varepsilon_N}}{\sigma_N^2} \end{bmatrix} \\
&= diag\left[\frac{\varepsilon_1}{\sigma_1^2}, ..., \frac{\varepsilon_N}{\sigma_N^2}\right] - \frac{\sum_{i=1}^{N} \frac{|\alpha_i|^2 \tilde{\varepsilon}_i^2}{(\sigma_i^2)^2 \varepsilon_i}}{\sum_{i=1}^{N} \hat{\varepsilon}_i \frac{|\alpha_i|^2}{\sigma_i^2}}.
\end{aligned}
$$

The channel coefficient vector ($[\mathbf{I}_{\boldsymbol{\alpha\alpha}}]^{-1}$) can be represented in condensed form:

$$[\mathbf{I}_{\boldsymbol{\alpha\alpha}}]^{-1} = var(\hat{\alpha}) = D_{i,j}\Big|_{\substack{i=1..N \\ j=1..N}}, \tag{35}$$

where N represents the total number of bands and each element $D_{i,j}$ is given by:

$$D_{i,j} = \begin{cases} \dfrac{\varepsilon_i}{\sigma_i^2} - \dfrac{\sum\limits_{i=1}^{N} \dfrac{|\alpha_i|^2 \tilde{\varepsilon}_i^2}{(\sigma_i^2)^2 \varepsilon_i}}{\sum\limits_{i=1}^{N} \hat{\varepsilon}_i \dfrac{|\alpha_i|^2}{\sigma_i^2}} & \text{if} \quad i = j \\ -\dfrac{\sum\limits_{i=1}^{N} \dfrac{|\alpha_i|^2 \tilde{\varepsilon}_i^2}{(\sigma_i^2)^2 \varepsilon_i}}{\sum\limits_{i=1}^{N} \hat{\varepsilon}_i \dfrac{|\alpha_i|^2}{\sigma_i^2}} & \text{if} \quad i \neq j \end{cases} \tag{36}$$

Location accuracy adaptation is dependent on the available bandwidth in the spectrum. According to (34), it is inherently impossible to extract the required bandwidth for a specific positional accuracy. Therefore the combining estimation technique in Section III has been proposed, which allows the extraction of the estimated required bandwidth and thus enables the positional accuracy adaptation feature for cognitive radio.

V. UHF Spectrum Occupancy Probability Density Function

According to [13], predefined discrete multiple bandwidths were utilised to perform 2D location estimation. Although an improved accuracy was observed, the study was limited in relation to a hypothetical fixed bandwidth availability model, which does not take into account of dynamic spectrum access. A realistic case would involve the cognitive radio device dynamically selecting multiple bandwidths based on availability to perform TOA positioning. Owing to the unpredictable nature of spectrum occupancy, the bandwidth availability would have to be modelled according to a particular type of PDF. As an initial starting point a PDF model would be derived based on the results obtained from a UHF spectrum occupancy measurement campaign conducted at the University of Pretoria campus. The objective is to determine the likelihood of available

(unoccupied spectrum holes) or unavailable (occupied spectrum holes) bandwidths and thereafter apply the PDF model to the multiband TOA positioning system. In the case of other frequency bands such as GSM, ISM, etc. the dynamic bandwidth availability model would surely differ and this would in turn affect the multiband TOA results. The UHF bands consist primarily of TV bands, which according to the IEEE 802.22 WRAN standard aims to provide broadband access to rural areas through the use of certain cognitive radio functionality. Although the empirical measurements are limited to one area, the results provide a reasonable validation to the performance of the proposed multiband TOA positioning model.

A. Measurement Campaign

A measurement campaign with the objective of assessing the spectrum occupancy of the UHF band in a South African context was conducted over a six-week period. The overall measurement system was based on the energy detection spectrum sensing scheme. Due to its low complexity and simplistic hardware implementation, it has been the preferred sensing technique in various spectral occupancy measurement campaigns [1], [2], [16], [17]. The measurement readings were obtained over the whole UHF frequency band, i.e. 470-854 MHz. The spectrum occupancy measurements were conducted on the rooftop of the 15-storey Engineering I building, University of Pretoria, Hatfield campus, which is regarded as a typical suburban area of Pretoria. The key spectrum occupancy measurement system components comprised of a UWB antenna (ranging from 25 MHz and 6 GHz), Agilent spectrum analyser, which was then connected to a workstation computer where sample data was remotely stored in a server accessible over the university's local area network. In order to quantify the occupancy of the band in question, a measurement scheduler was designed to analyse the data over a 24-hour period for several days. Each measurement reading consisted of 1500 samples and a sample comprised of an entire sweep of the band (384 points). The measurements were conducted at every two-hour intervals with a resolution of 1 MHz. Over the whole course of the measurement campaign approximately 170 million samples were collected.

B. PDF of the UHF Spectrum Occupancy

The raw measurements taken from the UHF measurement campaign were pre-processed and equalised in order to remove any outliers that can cause statistical inaccuracies. The basis of this method is to infer the spectral occupancy based on the noise statistics of the measurement readings. One problem that may arise, is that the received signal strength can be less than that of the noise floor, implying that an unoccupied channel is detected when in fact a signal is present. A histogram of all the sampled data over the whole measurement period for the UHF band was obtained and the probability density function of the received signal strength was plotted, as shown in Fig. 2.

According to the measurement results from Fig. 2, the occupied and unoccupied (noisy) portions of the UHF band are clearly distinguishable. The analysis of the unoccupied spectrum for the UHF band reveals that the probability distribution is Gaussian with a mean ($\mu_{uhf} = -90.2\ dBm$) and a standard deviation given by $\sigma_{uhf} = 1.0139$. The mean falls within the measured average system sensitivity, which was determined to be $-104.5\ dBm$ for the UHF band. The resulting probability distribution is utilised to model unoccupied channel bandwidth availability for performing TOA location estimation over multiple bands. Therefore, in this particular study, the PDF shown in Fig. 2 regarding UHF bandwidth availability applies to all multiple bands (sub-bands) and is characteristic of the environment in which the measurement campaign was undertaken.

VI. Simulation Results

A. Location estimation algorithms

The multiband positioning model was evaluated using three types of location estimation algorithms, viz. NLS, LLS and TSML. The NLS estimate ($\hat{\mathbf{m}}$) of the 2D position estimate corresponds to the minimum value of the cost function (Φ_{NLS}):

$$\hat{\mathbf{m}} = \arg\min_{\tilde{\mathbf{m}}} \Phi_{NLS}(\tilde{\mathbf{m}}), \tag{37}$$

where $\tilde{\mathbf{m}} = \begin{bmatrix} x & y \end{bmatrix}$ is the estimated 2D location coordinates of the target node (e.g. mobile cognitive radio device). The NLS cost function to be minimised for N anchor nodes (ANs) is given as:

$$\Phi_{NLS}(\tilde{\mathbf{m}}) = \sum_{i=1}^{N} \left(r_i - \sqrt{(x - x_i)^2 + (y - y_i)^2} \right)^2, \tag{38}$$

where $r_i = d_i + n_i$ is the corrupted TOA measurement from each AN, $b_i = \begin{bmatrix} x_i & y_i \end{bmatrix}$(e.g. cognitive radio base station) identified by i. The true distance between the AN and target node (TN) is given by $d_i = ct_i$ where t_i time delay of the signal while n_i represents AWGN. Faster convergence of the NLS estimation algorithm was achieved with the Newton-Raphson numerical method.

A global solution is achieved using the LLS and TSML linear methods in order to solve the location estimation problem, which results in lower complexity of the algorithms when compared to the NLS method. The LLS estimate is given by the expression [18]:

$$\hat{\boldsymbol{\theta}}_{LLS} = \left(\mathbf{A}^T \mathbf{A} \right)^{-1} \mathbf{A}^T \mathbf{b}, \tag{39}$$

where:

$$\mathbf{A} = \begin{bmatrix} x_1 & y_1 & -\frac{1}{2} \\ x_2 & x_2 & -\frac{1}{2} \\ \vdots & \vdots & \vdots \\ x_N & y_N & -\frac{1}{2} \end{bmatrix}, \tag{40}$$

and:

$$\mathbf{b} = \frac{1}{2} \begin{bmatrix} x_1^2 + y_1^2 - r_{,1}^2 \\ x_2^2 + y_2^2 - r_{,2}^2 \\ \vdots \\ x_N^2 + y_N^2 - r_{,N}^2 \end{bmatrix}. \tag{41}$$

The LLS vector estimate is given by:

$$\hat{\boldsymbol{\theta}}_{LLS} = \begin{bmatrix} x & y & R^2 \end{bmatrix}, \tag{42}$$

where x and y represent the estimated 2D coordinates of the TN while $R = \sqrt{x^2 + y^2}$ is an added dummy variable. Similarly, the TSML vector estimate is given by the following equation

[19]:

$$\hat{\boldsymbol{\theta}}_{TSML} = \left(\mathbf{A}^T \mathbf{A} \boldsymbol{\Psi}^{-1}\right)^{-1} \mathbf{A}^T \mathbf{b} \boldsymbol{\Psi}^{-1}, \tag{43}$$

where $\boldsymbol{\Psi} = diag\left\{4\sigma_1^2 d_1^2, 4\sigma_2^2 d_2^2, ..., 4\sigma_N^2 d_N^2\right\}$ represents the noise covariance matrix.

B. Results and Analysis

In order to realise the benefit of the proposed positioning technique for a cognitive radio device in a dynamic spectrum access scenario, a comparison is drawn between performing TOA estimation over a single-band and multiband system. In order to simulate dynamic bandwidth availability, 5 different bandwidths were randomly generated between 1 MHz and 10 MHz over a large enough sample according to a Gaussian distribution as determined for an unoccupied UHF spectrum in Fig. 2. The root mean square error (RMSE) of the positional accuracy was utilised to quantify the performance of the model at various SNRs. Therefore the RMSE was expressed as:

$$RMSE = \sqrt{\frac{\sum_{n=1}^{N}\left[(\hat{x}_n - x)^2 + (\hat{y}_n - y)^2\right]}{M}}, \tag{44}$$

where M represents the number of samples and $\begin{bmatrix} \hat{x}_n & \hat{y}_n \end{bmatrix}^T$ is the iterative position estimate each sample and x and y represent the actual coordinates of the TN. A priori information regarding the channel coefficients were assumed to be Rician distributed with K-factor of $2\ dB$. Figs. 3, 4 and 5 display the performance of the proposed technique in relation to the NLS, LLS and TSML algorithms respectively.

An improvement in location accuracy can be observed when performing multiband TOA estimation for all three different types of estimation algorithms. This is due to the fact that each band is characterised by a different time delay and channel fading coefficient and therefore all signal bandwidths can be exploited to yield an improved estimate. Table I shows the different percentages in RMSE improvement for the multiple discrete bandwidths at an SNR of 0 dB.

According to Fig. 3, 4 and 5, there is a significant RMSE positional accuracy improvement at lower SNRs. The proposed multiband TOA positioning technique can therefore be exploited

Table I
PERCENTAGE RMSE IMPROVEMENT OVER SINGLE-BAND SYSTEMS AT $SNR = 0\ dB$

	NLS (%)	LLS (%)	TSML (%)
Two bands	72	76	74
Three bands	88	81	77
Four bands	89	83	81
Five bands	90	84	82

in low SNR conditions to achieve an improved localisation accuracy. Table I also shows that there is a 1% performance improvement between utilising four and five discrete bandwidths for TOA positioning, which is a minimal improvement. Table II shows the comparative performance between the three location estimation algorithms at three different SNRs for the double band case.

Table II
COMPARATIVE ALGORITHMIC PERFORMANCE IN TERMS OF RMSE FOR TWO BANDS

	NLS (m)	LLS (m)	TSML (m)
-10 dB	115.5	52.59	42.76
-5 dB	25.30	23.82	20.15
20 dB	0.97	1.14	1.1

The TSML algorithm displays the best performance at lower SNRs. It can be observed that the more complex NLS algorithm performs slightly better than the LLS and TSML algorithm at higher SNRs. Table III shows the differential change in the RMSE of the positional accuracy between the single and double band case in order to quantify the improvement in accuracy. According to Table III, there is a significant decrease in RMSE for the double band case, especially between -10 dB and 0 dB, indicating a large improvement in positional accuracy. In the case of the NLS algorithm, there is a reduction in positioning error of three orders of magnitude between the -10 dB and 10 dB case owing to the accuracy of the initial estimate. Although the LLS and TSML algorithms display similar performances in terms of estimation accuracy, it can be noted that the TSML technique was slightly more complex to implement because of the addition of noise statistics. Therefore according to the results shown in Fig. 4 and 5, the LLS algorithm would be the most suitable choice of implementation. The proposed multiband positioning technique

is suitable for performing cognitive radio localisation of a SU in scenarios where high SNRs of the signal are limited by the inherent constraint imposed by the surrounding environmental conditions.

Table III
DIFFERENTIAL CHANGE OF THE RMSE FOR THE DOUBLE BAND CASE

	NLS (m)	LLS (m)	TSML (m)
-10 dB	7309.5	367.41	283.44
-5 dB	112.42	122.18	99.75
0 dB	49.63	37.75	41.15
10 dB	6.47	4.29	5.41
20 dB	1.52	1.76	1.59

VII. CONCLUSION

This study has considered a typical cognitive radio scenario where data from an energy-detection based measurement campaign provided a realistic view on the PDF of multiple bands which can be then exploited to perform TOA localisation. Derivations of the parameter estimates (time delay and channel coefficients) and combining estimation technique have also been provided. It has been shown through a statistical analysis of the UHF measurement data that the unoccupied portion of the spectrum adheres to a Gaussian distribution. The simulation results highlight the advantage of exploiting varying bandwidths in a dispersed and opportunistic manner at the cognitive radio receiver for improving positional accuracy. The LLS and TSML techniques have been shown to offer good performance with low complexity in terms of algorithm implementation.

ACKNOWLEDGEMENTS

This research work was financially supported by the Sentech Chair in Broadband Wireless Multimedia Communications at the University of Pretoria, the National Research Foundation and the Independent Communications Authority of South Africa.

REFERENCES

[1] Lopez-Benitez M, Casadevall F, Hachemani R, Palicot J. Spectral Occupation Measurements and Blind Standard Recognition Sensor for Cognitive Radio Networks. In: Proc. 4th Intl. Crowncom Conf. Hannover, Germany; 2009. p. 1–9.

[2] Chang RIC, Rowe GB, Sowerby KW. A Quantitative Analysis of Spectral Occupancy Measurements for Cognitive Radio. In: Proc. 65th IEEE Vehic. Technol. Conf. (VTC). Dublin, Ireland; 2007. p. 3016–3020.

[3] Fette B. 4. In: Cognitive Radio Technology. 1st ed. Elsevier-Newnes; 2006. .

[4] Stevenson CR, Chouinard G, Lei Z, Hu W, Shellhammer SJ, Caldwell W. IEEE 802.22: The First Cognitive Radio Wireless Regional Area Network Standard. IEEE Commun Mag. 2009 January;47(1):130–138.

[5] Arslan H, Celebi H. Utilisation of Location Information in Cognitve Wireless Networks. IEEE Wireless Commun Mag. 2007 August;14(4):6–13.

[6] Celebi H, Arslan H. Cognitive Positioning Systems. IEEE Trans Wireless Commun. 2007 December;6(12):4475–4483.

[7] Gezici S, et al. Localization via Ultra-Wideband Radios. IEEE Sig Process Mag. 2005 July;22(4):70–84.

[8] Qi Y, Kobayashi H, Suda H. On Time-of-arrival Positioning in Multipath Environment. IEEE Trans on Vehicular Technology. 2006 September;55(5):1516–1526.

[9] Mailaender L. Comparing Geo-location bounds for TOA, TDOA and Round trip TOA. In: Proc.18th IEEE Int. Symp. PIMRC. Athens; 2007. p. 1–5.

[10] Gezici S, Celebi H, Poor HV, Arslan H. Fundamental limits on time delay estimation in dispersed spectrum cognitive radio systems. IEEE Trans on Wireless Commun. 2009 Jan;8(1):78–83.

[11] Kocak F, Celebi H, Gezici S, Qaraqe KA, Arslan H, Poor HV. Time delay estimation in dispersed spectrum cognitive radio systems. Eurasip Journal on Advances in Signal Processing. 2010;2010:1–10.

[12] Farhang-Boroujeny B, Kempter R. Multicarrier communication techniques for spectrum sensing and communication in cognitive radios. IEEE Commun Mag. 2008 April;46(4):80–85.

[13] Thomas RR, Zayen B, Knopp R, Maharaj BT. Multiband TOA Positioning Technique for Cognitive Radio Systems. In: 22nd PIMRC Workshop on Cognitive Radio and Networking: Solutions and Challenges Ahead. Toronto, Canada; 2011. p. 2315–2319.

[14] Kay SM. 3. In: Fundamentals of Statistical Signal Processing, Volume 1: Estimation Theory. 1st ed. Addison Wesley Longman; 2001. .

[15] Proakis JG, Salehi M. 1. In: Digital Communications. 5^{th} ed. McGraw-Hill; 2008. .

[16] Wellens M, Wu J, Mahonen P. Evaluation of Spectrum Occupancy in Indoor and Outdoor Scenario in the Context of Cognitive Radio. In: Proc. 2nd Intl. Crowncom Conf.. vol. 4; 2006. p. 1658–1663.

[17] Qaraqe KA, et al. Empirical Results for Wideband Multidimensional Spectrum Usage. In: IEEE Symp. on Personal, Indoor and Mobile Radio Communications (PIMRC), 2009; 2009. p. 1262–1266.

[18] Chan YT, Ho KC. A simple and efficient estimator for hyperbolic location. IEEE Trans on Signal Process. 1994 August;42(8):1905–1915.

[19] Guvenc I, Chong C. A Survey on TOA based Wireless Localization and NLOS Mitigation Techniques. IEEE Commun Surveys and Tutorials. 2009 August;11(3):107–124.

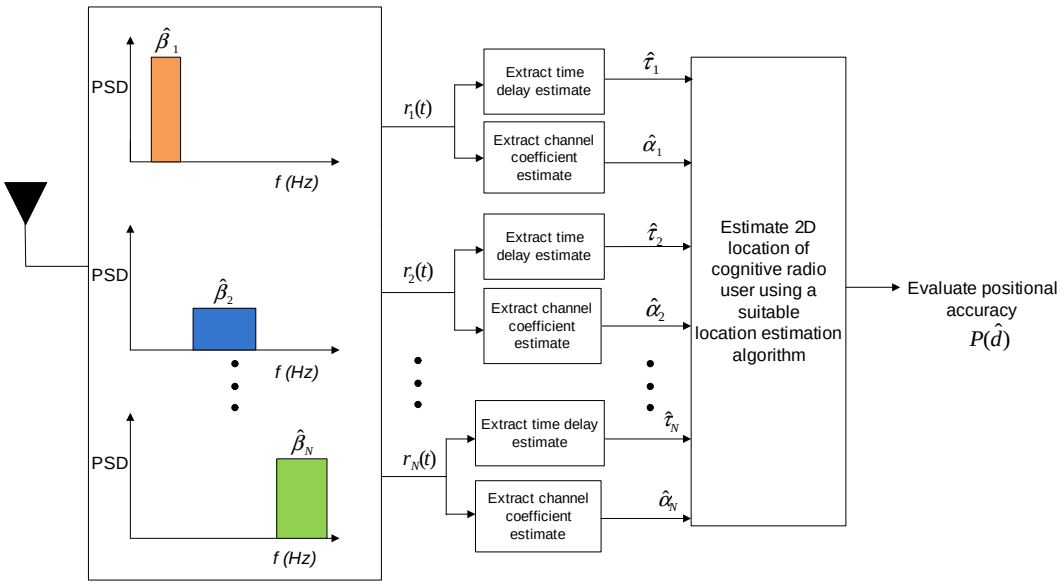

Figure 1. Multiband receiver model

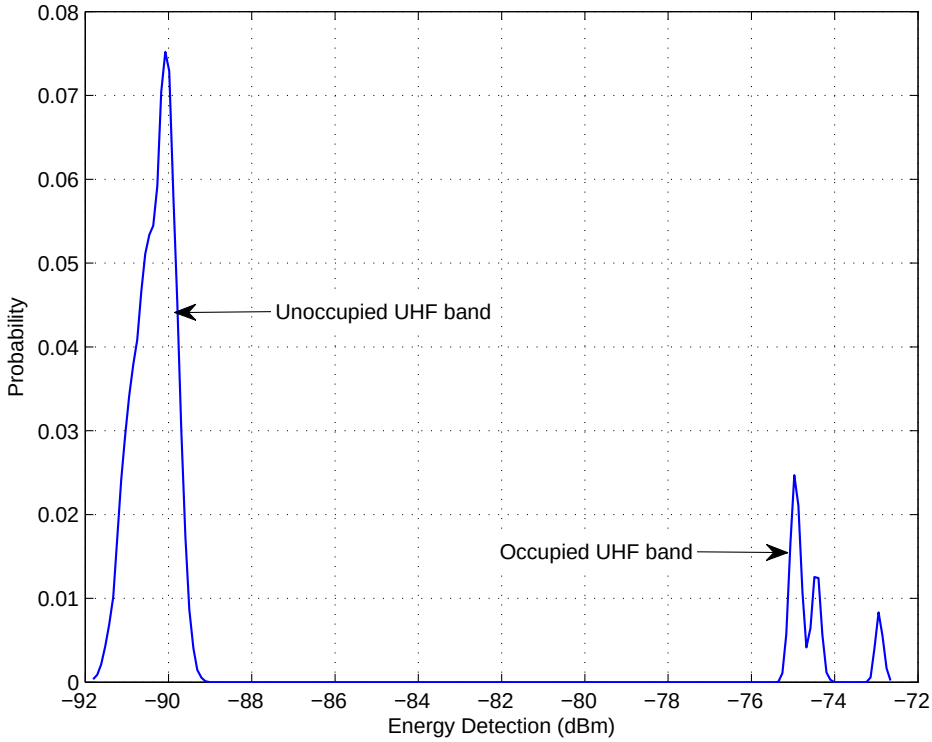

Figure 2. Probability density function of the received signal strength for the UHF band

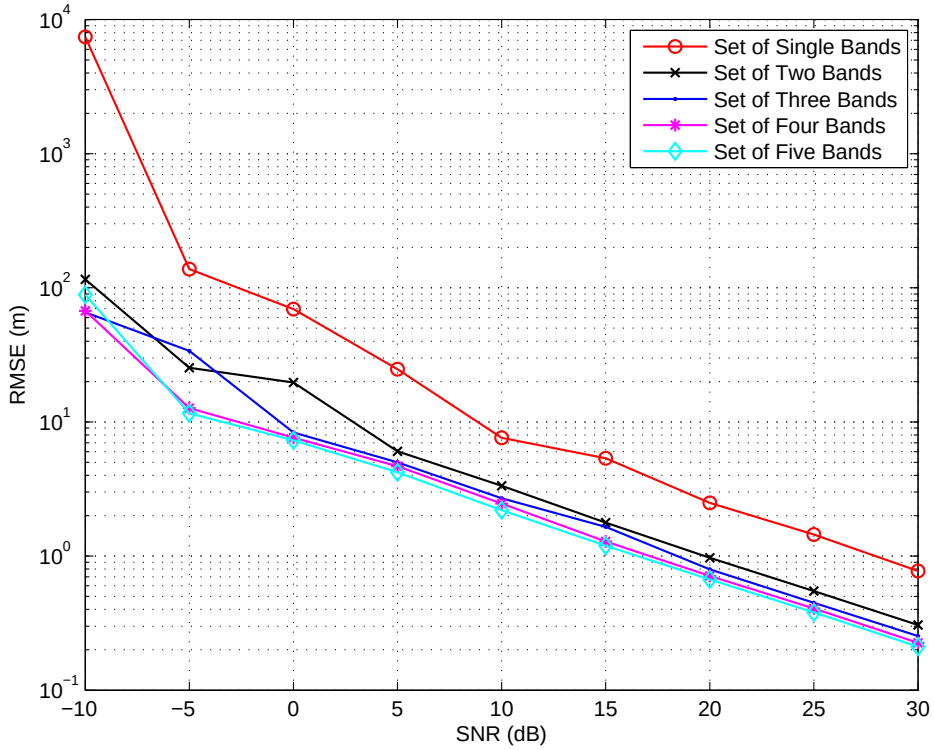

Figure 3. RMSE performance for the NLS algorithm

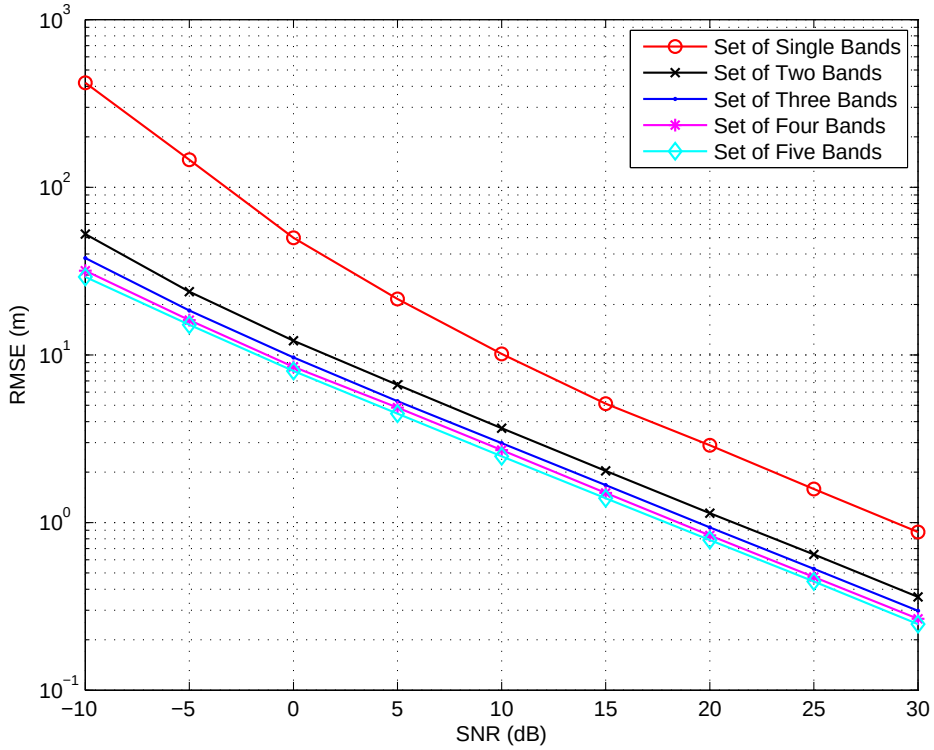

Figure 4. RMSE performance for the LLS algorithm

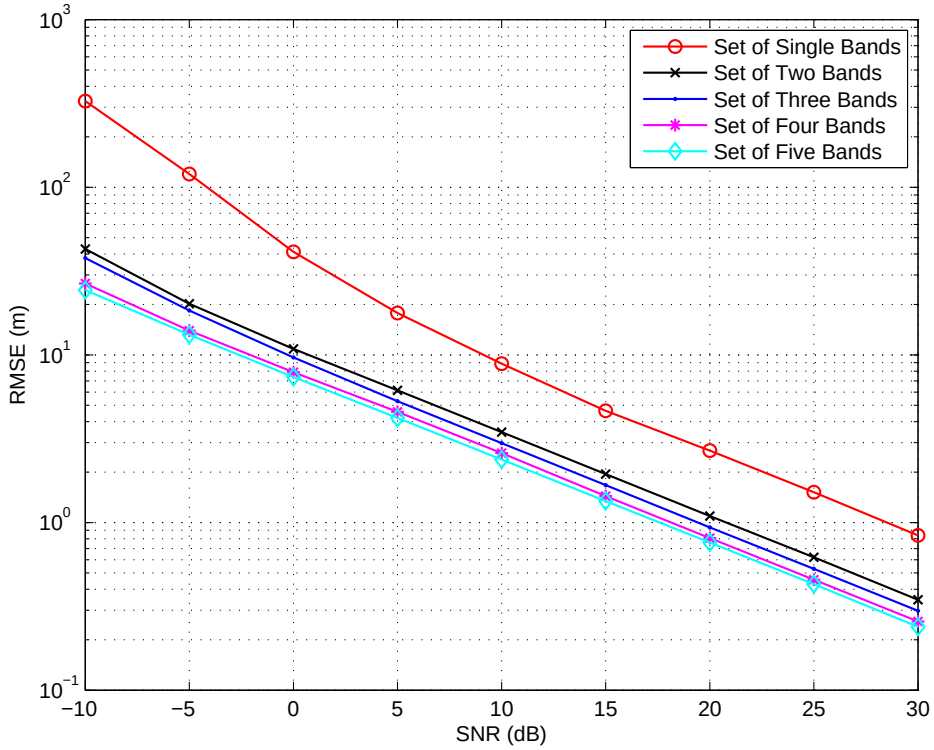

Figure 5. RMSE performance for the TSML algorithm